

## Propeller Design and Finding of Match-Point for Shallow-Fishery and Tailing Thai Boat : 3-Blade Type

J. Charoensuk<sup>1</sup>, J. Noosomton<sup>2</sup>

Faculty of Engineering, King Mongkut's Institute of Technology Ladkrabang, Bangkok, Thailand, 10520

<sup>1</sup>E-mail; kcjaruw@kmitl.ac.th, Tel. (66)-0-2326-9987, Fax. (66)-0-2326-9053

<sup>2</sup>E-mail; imcjrj@src.ku.ac.th, Tel. (66)-38-352606-10 Ext.2679, Fax. (66)-38-352607

### ABSTRACT

This paper presents the Propeller Design and Finding of Match-Point for Shallow-Fishery and Tailing Thai Boat, especially for 3-Blade type, in Thailand. The research concerns about the match-point and propeller shape designs of: I.) 3-blades narrow-developed area and II.) 3-blades width-developed area, by using NACA standards in the design and calculation procedures. The ultimate goal of this research is to offer an alternative model from existing design which rely on tacit experience of propeller-casting factory in Thailand, aiming to increase performance of propeller for shallow fishery ships and long-tailing Thai boat. The values of thrust coefficient ( $K_t$ ), torque coefficient ( $K_q$ ), break horsepower engine (BHP) are considered at various angle of attack ( $\alpha$ ), coefficient of advanced velocity ( $J$ ), Reynolds Number ( $Re$ ) and cavitations ( $\sigma$ ). These values of the new propeller design are analyzed to find the match point that suit for the application.

**Keywords:** Optimum Ship Propeller, Propeller Design, cavitations ( $\sigma$ )

### 1 INTRODUCTION

The design of new propeller for shallow-fishery and tailing Thai boat Type 3 Blades in Thailand, which has been expect to replace type local domestic. The propellers are more conditioned by the analysis of inception and developed cavitation. In recent years, the design has come increasing competitive together with a growing demand of heavily loaded propellers with request of very low noise and vibration levels onboard. Thus is the more important inhibitor to the propulsion system and it is comprehensive the need of a simple a fast method to predicted and

throughout increase performance of propeller for shallow fishery ships and long-tailing Thai boat. The values of thrust coefficient ( $K_t$ ), torque coefficient ( $K_q$ ), break horsepower engine (BHP) are considered at various angle of attack ( $\alpha$ ), coefficient of advanced velocity ( $J$ ), Reynolds Number ( $Re$ ) and cavitations ( $\sigma$ ). These values of the new propeller design are analyzed to find the match point that suit for the application, inclusion to predict cavitation behavior of the propeller in the design stage. As know, Cavitation flows are highly complicated because it is a rapid phase change phenomenon, which often occurs

in the high-speed or rotating fluid machineries. It is well known that the cavitating flows is of great interest. Numerical method is highly important approach for studying the cavitating flow. Computational methods for cavitation have been studied since over two decades ago. In general, the methods can be largely categorized into two groups, Single-phase modeling with cavitation interface tracking and multi-phase modeling with cavitation interface capturing.

The former approach has been widely adopted for in viscid flow solution methods, such as potential flow boundary element methods. It assumes the cavitation region as a large bubble with a distinct liquid/vapor interface. Basically three assumptions are made for a cavitation bubble; the bubble boundary is a free surface; the pressured inside the bubble is constant and equals to the vapor pressure of is corresponding liquid; the closure region of the bubble can be approximated by a wake model. Third assumption is prime limitation of the method. The computations ate done only for the liquid phase; grid is often regenerated iteratively to conform to the cavity shape. This method is capable of simulating sheer cavitation but may not be adequate for cases in which bubble growth and detachment exists. In addition they ate limited to two dimensional planar or axis-symmetric flows because of the difficulties involved in tracking three dimension interfaces, Kinnas and Fine (1993) developed non-linear boundary element method based on speed potential.

The latter approach can be adopted for viscous flow solution methods, such as the RANS equation solvers, and is very popular in the cavitation research recently. The cavitating flow is

treated as the homogeneous equilibrium single-fluid flow which satisfies Navier-Stokes equation. The key challenge is how to define the mixed density of the single-fluid. In general, the cavitation modeling can be largely categorized into two groups according the relation that defines the variable density field. One cavitation modeling is based on the equation of state that relates pressure can density. By assuming the cavitating process to be isothermal, mixed density is simply a function of local pressure. Hoeijmakers and Kwan (1998) adopted a sine law to simulate the cavitating flow around two dimensional hydrofoils with Euler equation, and the computational results of surface pressure coefficient are agreement with experimental data well Chen and Heister (1996) derived a time and pressure dependent differential equation for density. Qiao Qin (2003) used fifth order polynomial of pressure to define the mixed density. The other cavitation modeling is to introduce the concept to volume fraction, and then the mixed density is calculated using the volume fraction. Kubota et.al.,(1992) coupled the Rayleigh-Plesset equation to compute the volume fraction based on the bubble radius, A mass transport equation cavitation model has been recently developed Shin Hyung Rhee and Kawamura (2003) Studied the cavitating flow around a marine propeller using an unstructured mesh with FLUENT 6.1. The cavitating propeller performance as well as cavitation inception and cavity bubble shape were in good agreement with experiment measurements and observation. In addition, Francesco Salvatore (2003) developed a hybrid viscous/inviscous approach for the analysis of marine propeller cavitation.

## 2 DESCRIPTIONS AND NUMERICAL METHOD

### Description of Propeller Performance

Characterization; Dimensional Attributes:

Diameter [D] Overall diameter of the propeller

Rotation rate [N] rotational speed of the propeller in rps.

Density [ $\rho$ ] Fluid density

Thrust [T] Propeller axial thrust force

Torque [Q] Propeller shaft torque

Ship speed [ $V_s$ ] Ship velocity

Inflow velocity [ $V_a$ ] Mean inflow velocity

Non-Dimensional Characterization of propeller performance:

$$J = \frac{V_a}{ND}, \text{ Advance Coefficient.}$$

$$K_T = \frac{T}{\rho N^2 D^4}, \text{ Thrust Coefficient.}$$

$$C_T = \frac{2T}{\rho A V_a^2}, \text{ Thrust Coefficient. (A= Propulsion area)}$$

$$K_q = \frac{Q}{\rho N^2 D^5}, \text{ Torque Coefficient.}$$

$$\eta_o = \frac{T \cdot V_a}{2\pi N Q}, \text{ Propeller Efficiency}$$

$$\eta_t = \frac{R_t \cdot V_s}{2\pi N Q}, \text{ Propulsive Efficiency, (} R_t = \text{Total Ship resistance)}$$

### 2.1 Integral Formulation

Consider a right hands propeller rotating with constant angular velocity  $\omega$  in a axisymmetric incoming flow field  $V_\infty$  it same conclusion can be drawn for the simpler case of a wing subjected to an uniform inflow, neglecting the angular velocity term. In the  $(x_p, y_p, z_p)$  coordinate system that rotates with the propeller, the total velocity vector

$V$  can be written as the sum of the relative undisturbed inflow  $V_{rel}$  and the perturbation potential velocity  $q_{ind}$ , due to the velocity influence of the propeller itself on the velocity field:

$$V = V_{rel} + q_{ind} \quad (1)$$

Where the relative velocity  $V_{rel}$ , in the propeller reference system, can be written as:

$$V_{rel} = V_\infty - \omega \times r \quad (2)$$

With the assumption of an inviscid flow, irrotational flow and incompressible fluid, the perturbation velocity can be written in terms of a scalar function, the perturbation potential, which satisfies the Laplace equation:

$$q_{ind} = \nabla \phi, \quad \nabla^2 \phi = 0 \quad (3)$$

By applying Green's second identity for the perturbation potential, the differential problems (3) can be written in integral form with respect to the potential  $\phi_p$  at every point p laying on to the geometry boundaries. The perturbation potential  $\phi_i$  represents the internal perturbation potential, that must be set equal to zero in order to simulate fluid at rest inside the boundaries of all the bodies subject to the external inflow (Blade, hub).

$$2\pi\phi_p = \int_{S_B + S_{CB}} \left[ \phi_q - \phi_{q_i} \right] \frac{\partial}{\partial n_q} \frac{1}{r_{pq}} dS - \int_{S_B + S_{CB}} \left[ \frac{\partial \phi_q}{\partial n_q} - \frac{\partial \phi_{q_i}}{\partial n_q} \right] \frac{1}{r_{pq}} dS + \int_{S_w} \Delta \phi_q \frac{\partial}{\partial n_q} \frac{1}{r_{pq}} dS \quad (4)$$

When subscript  $q$  corresponds to the variable point in the integration,  $n$  is the unit normal to the boundary surfaces and  $r_{pq}$  is the distance

between points  $p$  and  $q$ . equation (4) expresses the potential on the propeller blade as a superposition of the potential induced by a continuous distribution of the sources on the blade and hub surfaces and a continuous distribution of dipoles on the blade, hub and wake surface that can be calculated, directly, via boundary conditions, or indirectly inverting equation (4).

## 2.2 Boundary Conditions

For the solution of equation (4) a certain number of boundary conditions must be applied. Different approaches are possible : a fully linear approach, in which cavity velocities can be considered enough small to allow linearization of boundary conditions or a fully nonlinear one, in which singularities are located on the cavity surface that need to be found iteratively. On the other hand, assumed on the wetted part of the body the kinematic boundary condition holds and allows to define the source strengths in terms of the known inflow velocity relative to the propeller reference system:

$$\frac{\partial \phi_q}{\partial n_q} = -V \cdot n_q \quad (5)$$

At the blade trailing edge the Kutta condition states that the flow must leave with a finite velocity or that the pressure jump at the blade trailing edge must be zero. In a steady problem, the Kutta condition allows to write the dipole intensities, constant along each streamlines, on

the wake, first, applying the “linear” Morino Kutta condition:

$$\Delta \phi_{T.E.} = \phi_{T.E.}^U - \phi_{T.E.}^L + V_{rel} \cdot r_{T.E.} \quad (6)$$

When the subscripts  $U$  and  $L$  stand for the upper and the lower face of the trailing edge. After, the zero pressure jumps can be achieved via an iterative scheme. In fact the pressure difference at trailing edge at each  $m$  streamlines is a non linear function of dipole intensities on the blade:

$$\Delta p_m(\phi) = P_m^U(\phi) - P_m^L(\phi) \quad (7)$$

## 2.3 Full Cavitation Model

The mixed density is controlled by vapor volume fraction  $f$ :

$$\frac{1}{\rho_m} = \frac{f}{\rho_v} + \frac{1-f}{\rho_l} \quad (8)$$

The vapor transport equation is written as:

$$\frac{\partial(\rho_m f)}{\partial t} + \nabla(\rho_m \bar{v} f) = \nabla(\mu_t \nabla f) + R_e - R_c \quad (9)$$

Where  $\rho_v$  and  $\rho_l$  are the density of vapor and liquid, respective,  $R_e$  and  $R_c$  are the rates of vapor generation and condensation, respectively. To solve the equation,  $R_e$  and  $R_c$  need to be given. Singhal et.al.(2002) derived the expressions of  $R_e$  and  $R_c$

$$R_e = -C_e \frac{\sqrt{k}}{S} \rho_l \rho_v \left( \frac{2}{3} \frac{p_v - p}{\rho_l} \right)^{\frac{1}{2}} (1 - f_v - f_g), \quad p < p_v \quad (10)$$

$$R_c = C_c \frac{\sqrt{k}}{S} \rho_l \rho_l \left( \frac{2}{3} \frac{p - p_v}{\rho_l} \right)^{\frac{1}{2}} f_v, \quad p > p_v \quad (11)$$

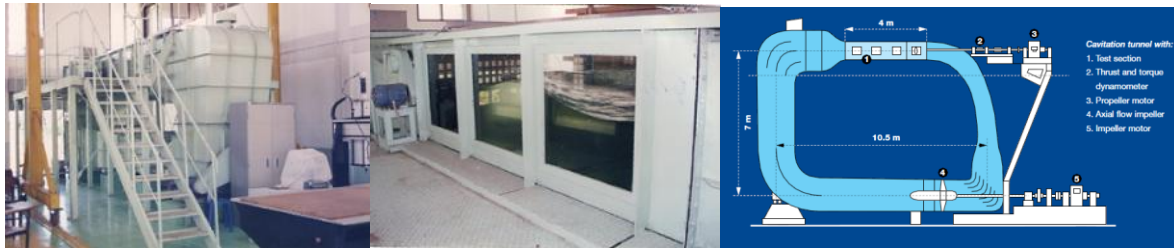


**Figure 1.** Lab. Water Tunnel and Draft Drawing

#### 2.4 Lifting Line Designed Propellers

In 1952, H W Lerbs<sup>[2]</sup> introduced a new method for calculating propellers named “lifting line”. Lerbs proposed to substitute the propeller blade with a so-called lifting line along which the radial distribution of lift is calculated under the influence of a number of trailing vortices. This was a new step forward in which the radial distribution of circulation (resembling lift or thrust) could be specified in order to obtain the optimum efficiency. An important difference from early days was the possibility to include the influence of the wake field. But the most consequential difference was the option to select profile section at each radius which could not only result in the optimum circulation/lift but which could also be selected with a combination of camber and pitch to achieve optimum cavitation performance, with the publication of the NACA airfoil sections. Series at almost the same time, a powerful tool was emerging, which for the first time could give the propeller designer a possibility to design a propeller with respect to cavitation aspects. See figure (2).

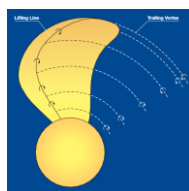


**Figure 2.** Principle of the “lifting line” calculation model<sup>[2]</sup>

Evaluation of the cavitation was facilitated by the work of T Brockett<sup>[3]</sup> who, for the above NACA airfoil sections, calculated a series of charts from which the onset of cavitation could be determined. Only the onset of cavitation could be calculated-not the degree of the chord-wise extension over the blade surface. As already mentioned a certain level of cavitation must regrettably be accepted on most merchant vessels in order not to compromise the efficiency too much. To overcome this obstacle, a method was devised by MAN B&W<sup>[4]</sup> to calculate the chord-wise distribution of lift by using a conformal mapping technique. As a result the cavitation could be a truly integrated part of the design process for the first time. One disadvantage of the lifting line model lies in the nature of the method. The substitution of the blade with a lifting line implies that the chord-wise extension of the lift is not directly included in the solution. After the appearance of the lifting surface method, a set of correction factors has been published<sup>[5,6]</sup> which can be incorporated into the lifting line model to improve the calculation accuracy.

#### 2.5 Lifting Surface Designed Propellers

An improvement of the lifting line model was developed in the 1980's (Greeley and Kerwin<sup>[7]</sup>) in an effort to overcome the shortcomings of the inadequate treatment of chord-wise lift of the

lifting line method as well as to include the influence of skew and rake. The method distinguishes itself from the lifting line, in the way it models the propeller blade. The surface of the blade is subdivided into a number of elements describing the surface, and on which a boundary condition of no through-flow is prescribed. To model the strength of the circulation/lift a distribution of vortices are located on the mean surface, and to include the effect of induced drag, a number of free trailing vortices are shed from each element. The method proved valuable in contribution to the understanding of skew and in particular its influence on pitch, camber and thickness which the lifting line had failed to do, without the inclusion of lifting surface correction factors. As with the lifting line method, the lifting surface method is sensitive as to how the trailing wake is modeled. This is especially important for heavily loaded propellers. See Figure (3).

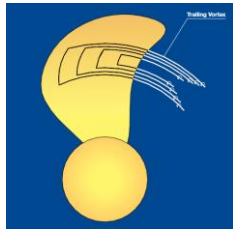


**Figure 3.** Principle of the “lifting surface” calculation model<sup>[2]</sup>

### 2.6 Blade Design

With all preconditions set the blade design can proceed. The main objectives within the constraint mentioned earlier is to obtain as high a TPE as possible and to suppress the cavitation to an acceptable level. However, for a fixed propeller diameter the only part-efficiencies being influenced by the blade design are the open water efficiency and the relative rotate efficiency.

It is a common belief among propeller designers that the two design objectives are in contradiction to each other and consequently must be balanced to get a compromised design. But today some design features are available which can be applied to reduce the cavitation without sacrificing the efficiency. To build up a propeller blade, the complicated 3-dimensional form is usually reduced into 2-dimensional elements which are then adjusted during the design process.

### 2.7 Blade area

The blade area should be kept as small as possible in order to reduce the friction losses when turning in the water, but to suppress the cavitation extension a certain area is needed. A measure of the blade area is the so-called “blade area ratio” ( $A_e/A_o$ ) which is the ratio of all the blades compared to the area of the circle circumscribed by the propeller diameter. See Figure (4).

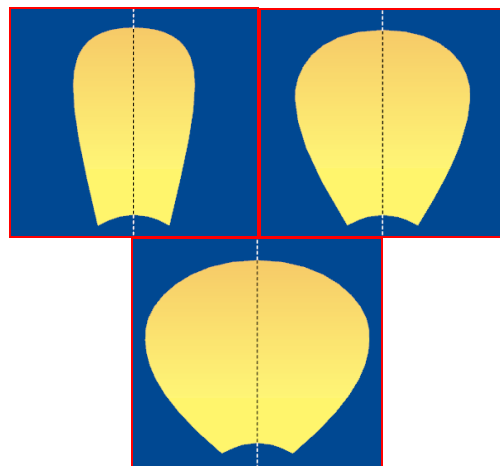


**Figure 4.** Different blade area ratios: Left:  $A_e/A_o=0.40$ , Center:  $A_e/A_o=0.55$ , Right:  $A_e/A_o=0.70$ <sup>[2]</sup>

## 2.8 Blade shape

The blade shape can be varied to even out the cavitation along radius and in the case of a nozzle propeller, it is advantageous to have wide-chord length at the tip (Kaplan shape). See Figure (5).

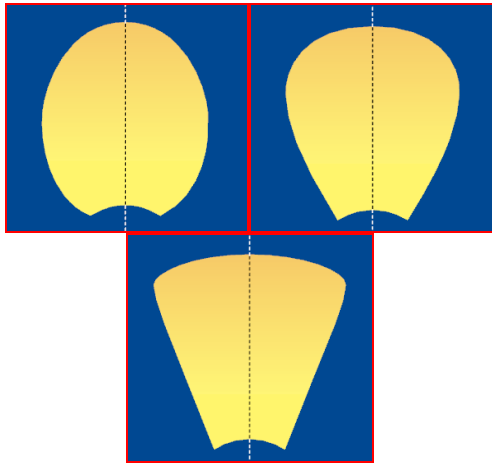


**Figure 5.** Different blade shapes, Max chord location varied from center of blade to tip of blade.<sup>[2]</sup>

## 2.9 Skew angle

A powerful tool to suppress propeller induced noise and vibration is the application of skew. For modern CP propellers, the skew distribution is of the balanced type, which means that the blade chords at the inner radii are skewed (moved) forward, while at the outer radii the chords are skewed aft. By applying this type of skew it is possible to control the forces (spindle torque) needed for pitch settings. In most cases the blades will be balanced in such a way that the forces in the design pitch setting will be zero. Skew has the advantage of reducing the pressure impulses emitted from propeller to the hull surface to as much as one third of an un-skewed design

without sacrificing the efficiency, which will remain unchanged. See Figure (6),(7).

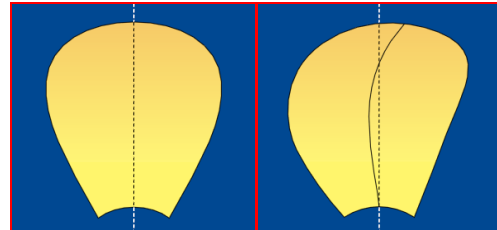


**Figure 6.** Left: Non Skew, Right: Low Skew<sup>[2]</sup>

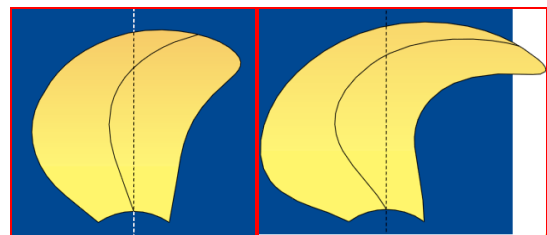


**Figure 7.** Left: Medium Skew, Right: High Skew<sup>[2]</sup>

## 2.10 Rake

The noise and vibration level in the aft ship depends on the distance between the propeller tip and hull surface - in particular exactly above and in front of the propeller. A way of increasing the distance is to rake (incline) the blade towards aft. As with skew the efficiency remains unchanged. However, the blade is exposed to higher stresses originating from an increase in the centrifugal forces which must be counteracted by an increase in blade thickness. See Figure (8).

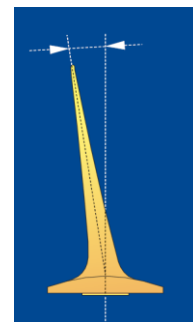


**Figure 8.** Aft raked propeller<sup>[2]</sup>

2.11 Profile section

For each radius, the blade is built-up of 2-dimensional airfoil sections. The airfoil used in propellers is mostly from the NACA family series which have proven successful in having both low drag and good cavitation characteristics. A NACA profile is characterized by a basic thickness and a camber distribution which can be changed independently of each other. This facilitates the design of profiles with specific properties at each radius. See Figure (9).

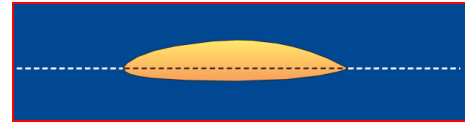
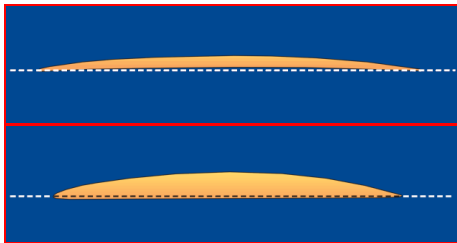


Figure 9. Typical profile sections at different propeller radii<sup>[2]</sup>

3 RESULTS AND DISCUSSIONS

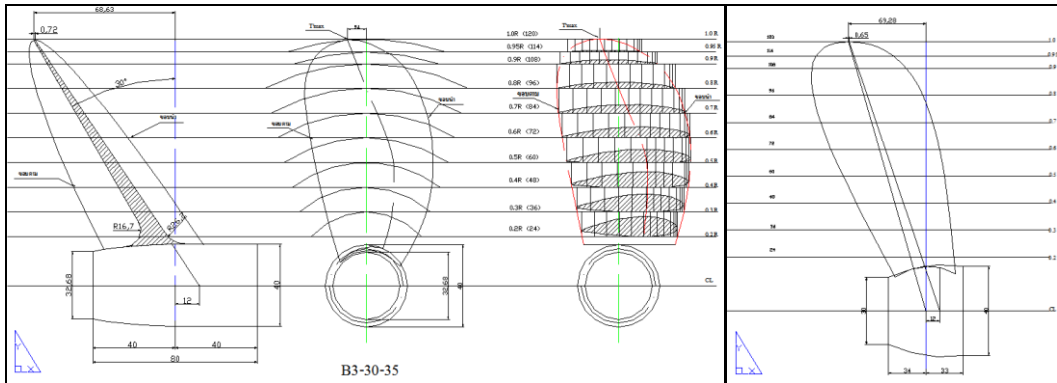
For validation of the numerical method, open water computational results are compared with the experimental data, which come from Francisco Pereira et.al.(2002) Table (1) presents the coordinate thickness of propeller blade with design for shallow-fishery and tailing Thai boat Type 3 Blades skew angle 30 degree developed area 35.

Table 1. Coordinate thickness of propeller blade Type B3-30-35 (New Design)

Backyard of Blade													
r/R	Trailing Edge					T'max	Leading Edge						
	100%	80%	60%	40%	20%		20%	40%	60%	80%	90%	95%	100%
0.95		0.32	0.52	0.63	0.70	0.72	0.70	0.64	0.52	0.32	0.21	0.16	
0.90		0.83	1.29	1.61	1.79	1.85	1.79	1.61	1.29	0.83	0.56	0.41	
0.80		1.22	2.02	2.54	2.88	2.98	2.89	2.54	2.04	1.44	1.03	0.76	
0.70		1.62	2.75	3.48	3.97	4.10	4.01	3.64	3.07	2.34	1.81	1.44	
0.60		2.10	3.51	4.47	5.06	5.23	5.13	4.77	4.15	3.33	2.73	2.27	
0.50		2.76	4.35	5.48	6.17	6.36	6.24	5.88	5.23	4.31	3.61	3.09	
0.40		3.57	5.26	6.48	7.26	7.49	7.35	6.98	6.31	5.27	4.50	3.91	
0.30		4.39	6.17	7.48	8.34	8.62	8.48	8.10	7.39	6.25	5.40	4.73	
0.20		5.20	7.08	8.47	9.25	9.74	9.61	9.21	8.48	7.25	6.27	5.55	
Front of Blade													
r/R	100%	80%	60%	40%	20%	T'max	20%	40%	60%	80%	90%	95%	100%
0.80						2.98							0.22
0.70						4.10					0.02	0.10	0.66
0.60	0.27					5.23				0.04	0.23	0.44	1.28
0.50	0.62	0.11				6.36			0.04	0.27	0.54	0.85	1.93
0.40	1.34	0.46	0.11			7.49		0.02	0.20	0.58	0.94	1.34	2.58
0.30	2.18	1.05	0.50	0.15		8.62		0.11	0.40	0.93	1.43	1.91	3.24
0.20	2.92	1.77	1.06	0.53	0.15	9.74	0.04	0.22	0.57	1.31	1.98	2.55	3.90

In figures (10),(12) show drawing design of new propeller type 3 blade skew angle 30° EAR 35 and 50 respective, for Figure (11),(13) was

propeller model for casting furnaces. This is after casting already it given new propeller for experimental.



**Figure 10.** Drawing Type 3 Blades Angle 30 Degree Developed Area 35; (B3-30-35) (New Design)



**Figure 11.** Illustration of propeller Model and Propeller casting Type B3-30-35 (New Design)

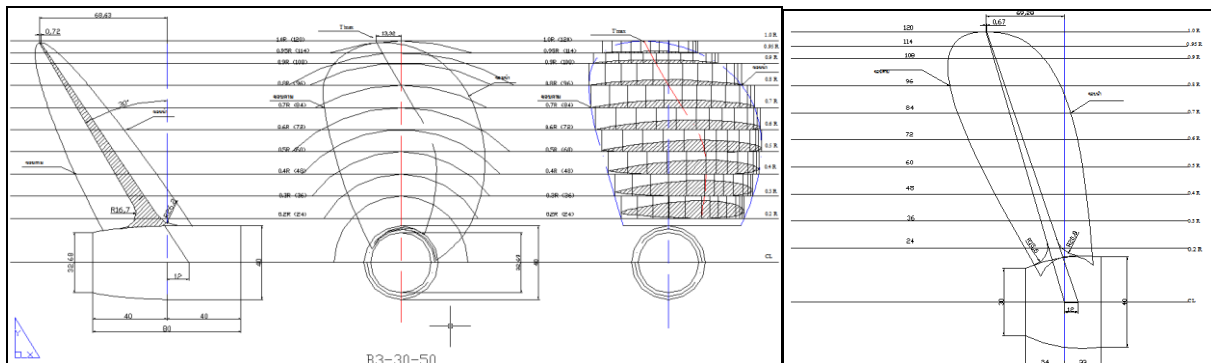


**Figure 12.** Drawing Type 3 Blades Angle 30 Degree Developed Area 50 (New Design)



**Figure 13.** Illustration of propeller Model and Propeller casting Type B3-30-50 (New Design)

The photographs in Figure.(14),(15) show cavity Appearance of propeller 3 blade skew angle 30 degree developed area 35,(B3-30-35) velocity speed 600 and 800 rpm. Respective,

Type new design for Shallow-Fishery and Tailing Thai Boat, An example of sequence by camera at the time when impulsive force was measured.



**Figure 14.** Illustration of propeller cavitation type B3-30-35 Velocity 600 rpm. (Tank Test)

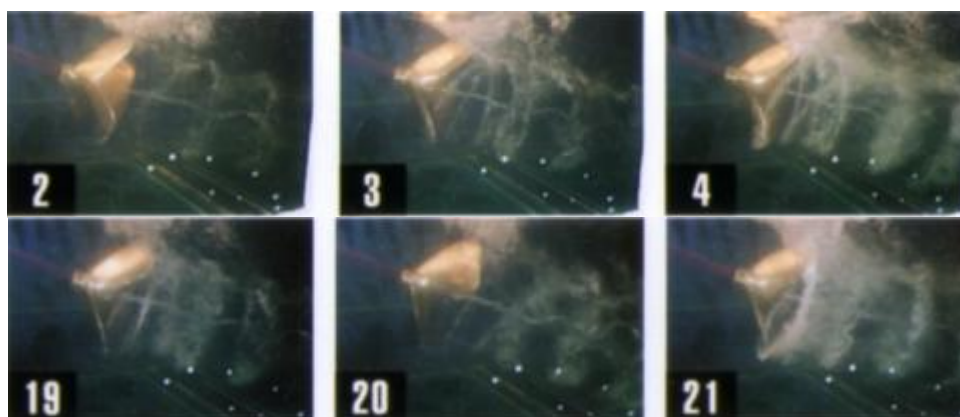


**Figure 15.** Illustration of propeller cavitation type B3-30-35 Velocity 800 rpm. (Tank Test)

The photographs in Figure.(16),(17) show cavity Appearance of propeller 3 blade skew angle 30 degree developed area 50,(B3-30-50) velocity speed 600 and 800 rpm. respective,

Type new design for Shallow-Fishery and Tailing Thai Boat, An example of sequence by camera at the time when impulsive force was measured.

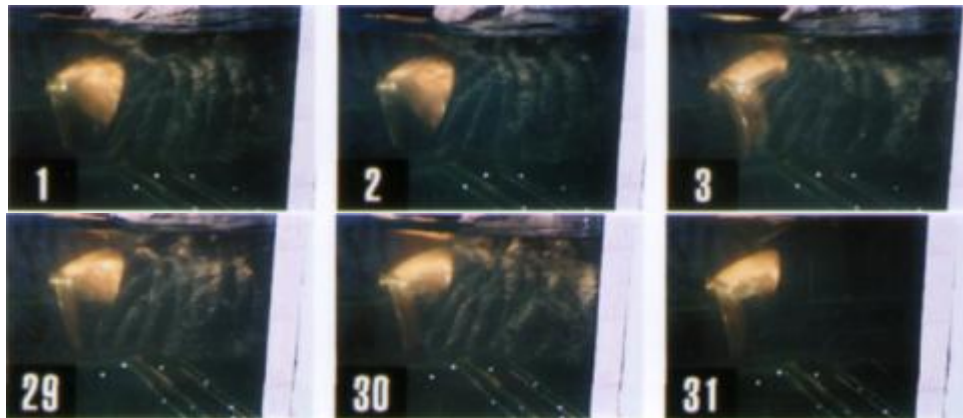


**Figure 16.** Illustration of propeller cavitation type B3-30-50 Velocity 600 rpm. (Tank Test)



**Figure 17.** Illustration of propeller cavitation type B3-30-50 Velocity 800 rpm. (Tank Test)

#### 4 CONCLUSIONS

An elucidate the bursting phenomenon of tip vortex cavitation, with experiments in a water tunnel and numerical simulation were carried out with two propellers, (B3-30-35, B3-30-50) and different thrust coefficients and cavitation numbers. The results obtained suggest that, large pressure fluctuations was measured twice in a series showing the bursting phenomenon in one rotation of propeller blade. In the first bursting tip vortex cavitation from the preceding blade interfere the sheet cavity, and that made the sheet cavity unstable and its trailing edge swelled significantly. When the sheer cavity was shed to the tip vortex cavitation and a vortex cavity from the trailing edge of the sheer cavity intertwined

with each other, causing implosion and rebound again and again. At this time, the tip vortex cavitation was spitted into many bubbles, and a bubble cluster, including small vortex cavities, formed. In the second, bursting occurred when the following blade approached upstream of the vibrating vortex, which had been intensely disturbed in the first bursting. The following blade swiftly obstructed the flow and caused tip vortex cavitation implosion and rebound again, and at that time bubbles in the tip vortex cavitation collapsed repeatedly and randomly.

The experiment has been considered to reduce the fluctuating pressure caused by bursting. One is to stabilize the tip vortex cavitation, and the other is to reduce the

cavitation itself. The occurrence of tip vortex cavitation can be predicted by the rate of change of the tip vortex intensity. The bursting occurs because the rate of change of the tip vortex intensity is related to the stability of the tip vortex.

## REFERENCES

- [1] Kuiper G., "The Wageningen Propeller Series.", Marin publication 92-001.,1992
- [2] Lerbs H.W, "Moderately loaded propellers with a finite number of blades and an arbitrary distribution of circulation.", SNAME Transaction, 60:73-117.,1952
- [3] Brockett, "Minimum pressure envelopes for modified NACA-66 sections with NACA a=0.8 camber and Buships type I and type II sections.", David Taylor Model Basin report 1780, 1966.
- [4] Nielsen J.R., "Program documentation. MAN B&W", internal document, 1992.
- [5] Morgan W.B., Silovic V., Denny, "Propeller lifting-surface corrections", SNAME Transaction 76:307-347.,1968
- [6] Cumming R.A., Morgan W.B., Boswell, "Highly skewed propellers", SNAME Transaction, Vol.80,1972
- [7] Greeley D.S., Kerwin J.E., "Numerical methods for propeller design and analysis in steady flow", SNAME Transaction 90: 415-453.,1982
- [8] A.H. Techet. Prof, "Hydrodynamics Reading", Version 3.0, pp.1-19, 2005
- [9] Bal S., Kinnas S.A., "A BEM for the prediction of free surface effects on cavitating hydrofoils"., computational Mechanics (28), 2002
- [10] Young Y.L., Kinnas S.A., "A BEM for the prediction of unsteady midchord face and/or back propeller cavitation", Journal of fluids engineering, Vol.123, 2001
- [11] Vaz G., Bosschers J., "Modeling three dimensional shear cavitation on marine propellers using a boundary element method", 6th international symposium on cavitation, The Netherlands, 2006
- [12] Bin Ji. et. Al., "Numerical investigation of unsteady cavitating turbulent flow around a full scale marine propeller", 9<sup>th</sup> international conference on hydrodynamics, Shanghai China, Oct 11-15, 2010
- [13] Nabil H. Mostafa, Mohammed A. Boraey, "Numerical and experimental investigation of cavitation in axial pumps", 8<sup>th</sup> international water technology conference, IWTC11, Sharm El-Sheikh Egypt, pp.553-564, 2007
- [14] R. Arazgaldi, A. Hajilouy, B. Farhanieh, "Experimental and numerical investigation of marine propeller cavitation", Scientia Iranica, Vol.16, No.6, pp.525-533, 2009
- [15] Akihisa Konno et.al., "On the mechanism of the bursting phenomena of propeller tip vortex cavitation", Journal of Marine Science and Technology,6:181-192, 2002

## ACKNOWLEDGEMENTS

The authors would like to thank Capt.Sarawut Wongchenyour; Royal Thai Navy for contributions toward this work. This work is supported by ANSYS Software at KMIT'L.